Environ Monit Assess (2007) 129:295–308
DOI 10.1007/s10661-006-9362-y

Assessment of Chlorophyll-*a* Concentration and Trophic State for Lake Chagan Using Landsat TM and Field Spectral Data

Hongtao Duan · Yuanzhi Zhang · Bai Zhang · Kaishan Song · Zongming Wang

Received: 11 March 2006 / Accepted: 28 June 2006 / Published online: 21 October 2006

Abstract In this study, we present the digital evaluation of Landsat TM data and field spectral measurements for retrieving chlorophyll-*a* (chl-*a*) concentration and trophic state index in Lake Chagan of Northeast China. Chl-*a* concentration of the lake can be estimated from the band ratio (TM4/TM3) and the field spectral data at 670 nm (absorption peak) and at 700 nm (reflectance peak). The results show that the best determination coefficient (R^2) is 0.67 from the TM data, by which chl-*a* distribution can be mapped. Based on chl-*a* determination from laboratory analysis, field spectral and TM data, the modified trophic state index (TSI_M) was applied to assess the lake's trophic state. With the available data in Lake Chagan, each algorithm demonstrates the similar result for assessing the lake's chl-*a* and trophic state. Our results indicate that Landsat TM and field spectral data could be used effectively to determine chl-*a* concentration and evaluate the trophic state of Lake Chagan in the study.

Keywords Chl-*a* · Trophic state · Spectral measurements · Landsat TM

H. Duan · B. Zhang · K. Song · Z. Wang
Northeast Institute of Geography and Agricultural Ecology,
Chinese Academy of Sciences,
Changchun 130012, China

H. Duan
Graduate School of Chinese Academy of Sciences,
Beijing 100039, China

Y. Zhang (✉)
Laboratory of Space Technology,
Helsinki University of Technology,
P.O. Box 3000, FIN-02015 HUT Espoo, Finland
e-mail: yuanzhi.zhang@hut.fi

1 Introduction

Lakes are valuable water resources and used for fishing, transportation, agriculture, industry, recreation and tourism. Up to the present, the water quality of a number of lakes around the world is so bad that it is almost unrecoverable by natural means of purification. The most commonly ecological problem of inland water bodies is the anthropogenic eutrophication. The change of water quality conditions is always resulted from economic development and sewage treatment. It has become the most widespread water quality problem in China and many other countries (Chen, Zhang, Ekroos, & Hallikainen, 2004; Giardino, Pepe, Brivio, Ghezzi, & Zilioli, 2001; Wang, Xia, Fu, & Sheng, 2004; Zibordi, Melin, & Berthon, 2006). For this reason, the issues of water quality deterioration and eutrophication have been acquired more and more attention from the public and government, and thus many studies have been carried out on lakes' water trophic state assessment (Brezonik, Menken, & Bauer, 2005; Dekker & Peters, 1993; Iwashita, Kudoh, Fujii, & Nishikawa, 2004; Xing, Guo, Sun, & Huang, 2005).

Chlorophyll-*a* (chl-*a*) is an important parameter to determine the lake trophic state. It is one major factor affecting water environment, and produces visible changes in the surface of waters (Ritchie, Cooper, & Schiebe, 1990; Zhang, Koponen, Pulliainen, & Hallikainen, 2002, 2003a, 2003b). Since it exists in all algae groups in marine and freshwater systems, chl-*a* concentration is a key indicator for bio-production of inland water bodies.

The trophic state index is a vital factor to evaluate the conditions of water quality. Walker et al. (e.g., Aizaki, Iwakuma, & Takamura, 1981; Porcella, Peterson, & Larsen, 1980; Walker, 1979) proposed 0–100 scale continuous numerical classes of lakes trophic states and a rigorous foundation for quantitative studies of the mechanisms behind lakes eutrophication. This effectively eliminates the subjective labeling associated with the use such oligotrophic, mesotrophic and eutrophic states as indicators (Xu, Shu, Dawson, & Li, 2001). Carlson (1977) suggested the most suitable and acceptable method for evaluating inland lake's eutrophication. However, due to various geographic sites, environment and human activities, the assessment methods for the types of lakes eutrophication are different. Such differences require researchers looking for a suitable method to assess the state of Chinese lakes eutrophication. Shu (1990, 1993) investigated 24 representative lakes and proposed a modified method fitting for the Chinese lakes eutrophication assessment based on Carlson's

Figure 1 Location of Lake Chagan in Jilin province, China.

Table I Sample number and chl-*a* contents and Secchi disk depth in different months of 2004

	May	June	July	August	September	October
Point number	11	6	8	9	20	20
Chl-*a* ($\mu g/l^{-1}$)						
Min	6.34	6.40	28.14	15.15	11.24	10.68
Max	19.13	14.68	58.21	37.15	47.23	28.68
Mean	14.26	10.22	40.57	28.81	24.38	20.91
SDT (m)						
Min	0.09	0.10	0.22	0.22	0.18	0.10
Max	0.30	0.46	0.24	0.30	0.32	0.27
Mean	0.14	0.25	0.23	0.25	0.25	0.14

modified trophic state index TSI_M (Aizaki et al., 1981). In this study, we examined this assessment method to evaluate the trophic status of Lake Chagan.

On the basis of *in situ* measurements or laboratory analysis of water samples, traditional water quality monitoring is crucial for any effort to produce information in support of water conservation and decision-making (Brivio, Giardino, & Zilioli, 2001; Ostlunda, Flinka, Strombeckb, Piersonb, & Lindell, 2001). Since monitoring normally needs to be carried out as cost-effectively as possible relative to the type of information needed, it is often expected that water quality should be shown with high accuracy in all places, in spite of the fact that direct observations can only be done in a limited number of locations. The need for an effective operational monitoring system able to solve the contradiction between cost-effectiveness and spatially comprehensive coverage is especially pronounced in areas with variable lakes and water flow conditions (Erkkila & Kalliola, 2004).

Satellite-based observations provide a suitable means to integrate limnological data collected from traditional *in situ* measurements (Giardino et al., 2001). However, satellite measurements cannot be independently analyzed using specific absorption characteristics due to its broad bandwidths. Hence, additional use of *in situ* samples and field spectral data can assist in finding new methods and improving the accuracy of chl-*a* estimation (Thiemann & Kaufmann, 2000).

In this study, Landsat TM and field spectral data were used to estimate chl-*a* concentration in Lake Chagan of Northeast China. Based on chl-*a* determi-

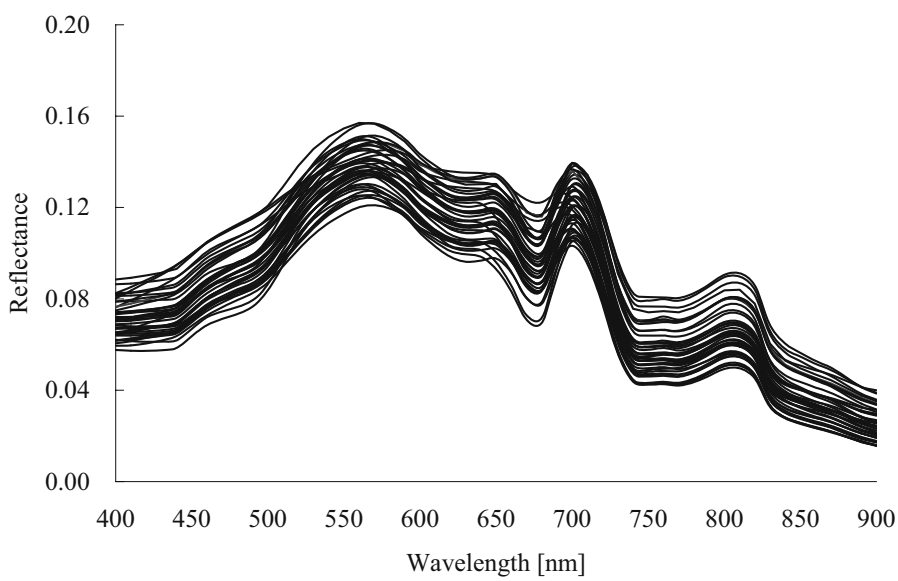

Figure 2 Reflectance spectra over Lake Chagan.

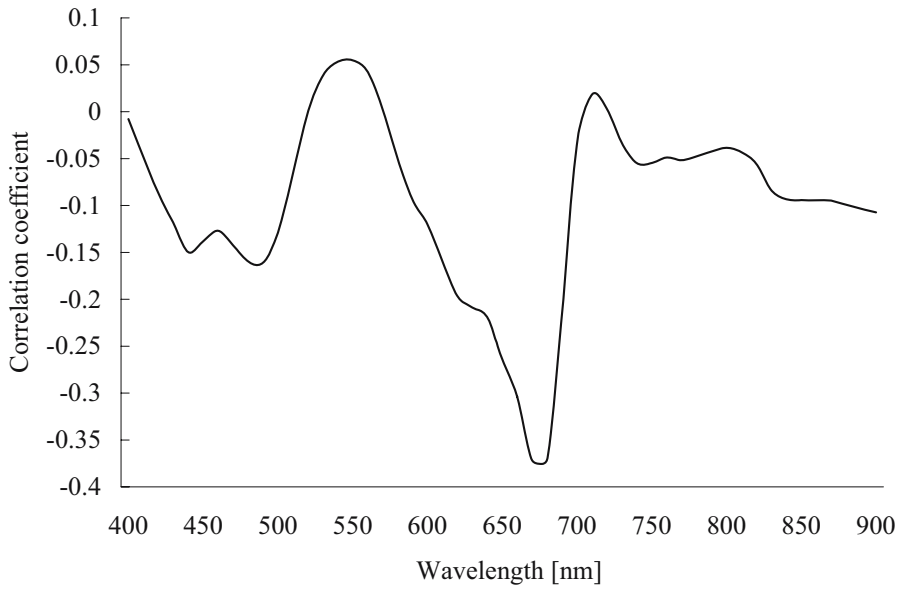

Figure 3 Correlation between chl-*a* content and single band spectral.

nation, the modified trophic state index (TSI_M; Shu, 1990, 1993) was applied to assess the lake's trophic status in the study area.

2 Study Area and Materials

2.1 Study area

Lake Chagan, located in the northwest of Jilin province in Northeastern China (see Figure 1), is one of the 10 largest fresh-water lakes in China. It has a mean surface area of 372 km^2, a mean depth of 2.52 m, and the largest storage capacity of 5.98×10^8 m^3. The lake is also one of eutrophic lakes in China with a high chl-*a* content and low Secchi disk transparency (SDT): chl-*a* is between 6 and 60 μg/L and SDT varies from 0.09 to 0.46 m (Table I). Songhua River is the main water supply for Lake Chagan.

The lake's primary economic value is linked to fishery, but it is also important for agriculture and recreational uses, and therefore a long-term of monitoring program for the lake's conservation is still needed.

2.2 Water sampling data

Water sampling and measurements were performed monthly from May to October 2004, and the monitoring frequency was once a month. Sampling number varied from 6 to 20 in different months (see Table I). The position of the sampling boat was geolocated by a portable global positioning system (GPS). SDT and field spectral data were simultaneously measured on site. At each sampling site, the lake water was collected with a clean bottle for the further analysis in the laboratory. The parameters chosen for measurement included physical parameters (e.g., turbidity, SDT, and total suspended matter) and chemical parameters (e.g., chl-*a*, pH, TN, TP, COD, BOD, and DO). In this study, chl-*a* content was mainly analyzed and assessed, while other parameters were accessorially used.

Table II Regressive equations and relation coefficients indicating the relationship between chl-*a* content and spectral reflectance ratios

Band ratio	Regressive equation	R^2	Band ratio	Regressive equation	R^2
710/440	$y = 42.805x - 41.959$	0.20	810/670	$y = 44.677x - 6.539$	0.19
710/670	$y = 78.018x - 65.88$	0.64	750/670	$y = 42.154x - 1.041$	0.15
700/670	$y = 93.67x - 90.40$	0.69	560/440	$y = 27.386x - 26.903$	0.14
710/680	$y = 74.782x - 64.065$	0.62	700/680	$y = 88.274x - 86.206$	0.67

2.3 Satellite data and field spectral measurements

One scene of Landsat TM was obtained on 14th October 2004 when the composition of the lake water was relatively stable during the dry season in the region. This TM image was cloud-free and with very good quality. Using ground control points (GCPs), the TM image was geometrically corrected using ENVI software. The TM was also re-sampled using the nearest neighbor method to preserve radiometry.

At the same time of TM data received, field spectral measurements and acquisition of *in situ* data

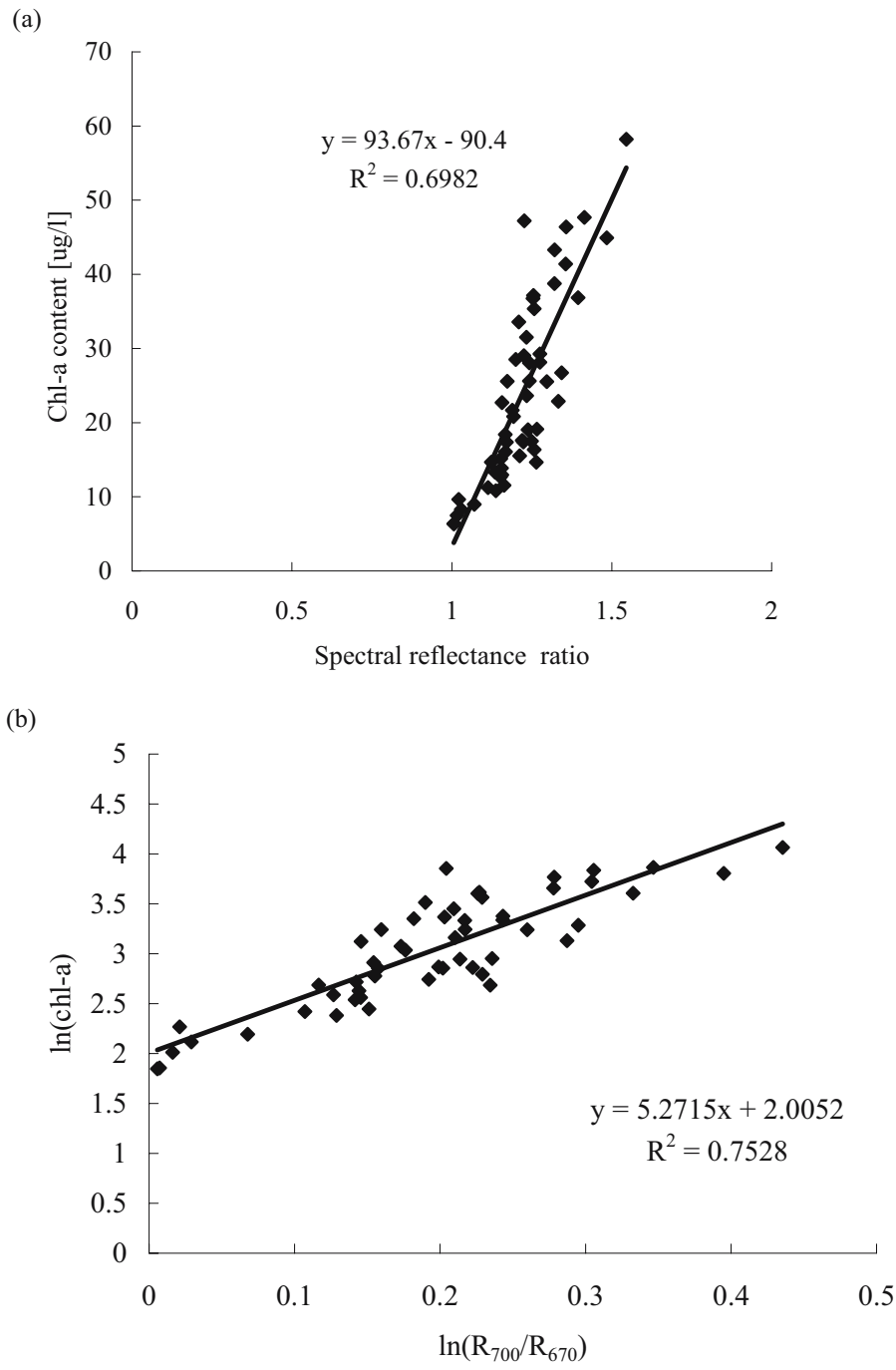

Figure 4 (a) Correlation between chl-*a* and spectral reflectance using the reflectance ratio at 700 and 670 nm. (b) Correlation between logarithmic chl-*a* and logarithmic spectral reflectance using the reflectance ratio at 700 and 670 nm.

were performed in several test-sites. Field spectra were measured with a portable Fieldspec FSR VNIR® spectrometer (ASD Inc.). The ASD radiometer has a spectral range between 350 and 1,100 nm. Its spectral resolution is about 3 nm. The measurements were taken from the boat platform above the lake surface about 1 m in the vertical downward direction. The measuring position was oriented to the boat side within the light propagation to minimize sun glint from waves, but far away from the effect of the boat shadow.

3 Methods

3.1 Spectral characteristics of chl-*a*

Chl-*a* is a phytoplankton pigment existing in all algae groups of inland waters. Figure 2 shows reflectance spectra for the eutrophic Lake Chagan in different months with various chl-*a* concentrations. They are common for inland water bodies of different trophic states. The resultant spectrum reveals a low reflectance value at the range of the wavelengths less than 500 nm, which is due to absorption by both algal pigments (e.g., chl-*a*) and dissolved organic matter (Gitelson et al., 1993). Because of the influence from suspended matter, the absorption peak of the phytoplankton pigments at 440 nm is not clearly visible. A linear reflectance increase exits between the wavelengths from 510–620 nm, which is resulted from low absorption due to phytoplankton pigments, coupled with an increase in backscattering when particle concentration increases. There are two minima of reflectance at near 630 and 670 nm. These correspond to the absorption maxima of phytoplankton pigments (Gitelson et al., 1991). Low reflectance at 630 nm is expected, due to absorption by cianopycocyanine. At 670 nm, a reflectance minimum corresponds to the chl-*a* absorption. A reflectance peak is obviously notable at 685–715 nm. This is due to fluorescence caused by chl-*a* pigments (Gordon, 1979). And in productive mesotrophic and eutrophic areas with the increase of chl-*a*, this peak leads to a shift of reflectance maximum toward the longer wavelengths (Gitelson et al., 1993). It reaches at 700 nm for the increase of chl-*a* concentration in Lake Chagan. Therefore, it should be highlighted that this peak is a unique spectral feature of phytoplankton (Arenz et al., 1996). All spectra shown in Figure 2 were also regarded more closely for the evaluation of the TM data.

3.2 Evaluation of field spectra regarding chl-*a*

The use of channel ratios for a relationship between remote sensing measurements and ground truth data is quite common. The advantage of using ratios over absolute values of reflectance is that they may correct some of the effects of measurements geometrically and atmospherically (e.g., Koponen, Pulliainen, Kallio, & Hallikainen, 2002; Koponen et al., 2001; Pulliainen et al., 2001). The most common chl-*a* algorithm has been the reflectance ratio between two channels in the region of 670–720 nm (Kallio et al., 2001),which can enlarge the differences between the absorption peak and the reflectance peak of chl-*a*. Previous studies (Dekker, 1993; Gitelson & Kondratyev, 1991) found a good correlation of chl-*a* with the ratio of 705 nm over 675 nm.

In this study, the best retrieval algorithm for each variable was found empirically by deriving a regression model for all possible bands and/or band ratio, and selecting the one with the highest correlation coefficient (R^2). The employed algorithms and their parameters are presented in Figure 3 and Table II. Our analyses with wavelength positions in the absorption and reflectance maximum resulted in almost the same good relationship as found by previous studies. However, absorption peak and reflectance maximum have a shift in Lake Chagan. That is, the absorption peak is at 670 nm and the reflectance maximum is at 700 nm in the study.

In some cases logarithmic transformation of variables increased the goodness of fitting for the model (Harma et al., 2001). Transformations complicate

Table III Thematic Mapper specifications

Band	Description	Spectral resolution wavelength (μm)
TM1	Visible blue-green	0.45–0.52
TM2	Visible green	0.52–0.60
TM3	Visible red	0.63–0.69
TM4	Near infrared	0.76–0.90
TM5	Infrared	1.55–1.75
TM6	Thermal infrared	10.40–12.51
TM7	Infrared	2.08–2.35

Table IV TM band 1–4 and their combinations in correlation with chl-*a* content represented in correlation coefficient (R) and the coefficient of determination (R^2)

Variables	R	R^2	Variables	R	R^2
TM1	0.51	0.26	AVERAGE (1, 2, 3)	0.55	0.31
TM2	0.62	0.38	AVERAGE(1, 2, 4)	0.70	0.50
TM3	0.40	0.16	AVERAGE(2, 3, 4)	0.66	0.44
TM4	0.78	0.62	AVERAGE(1, 3, 4)	0.65	0.43
TM4/TM1	0.73	0.54	AVERAGE(1, 2, 3, 4)	0.65	0.43
TM4/TM2	0.76	0.59	TM1*TM2	0.60	0.37
TM4/TM3	0.81	0.67	TM1*TM3	0.50	0.25
TM3/TM2	−0.38	0.15	TM1*TM4	0.77	0.60
TM3/TM1	−0.08	0.01	TM2*TM3	0.53	0.28
TM2/TM1	0.20	0.04	TM2*TM4	0.77	0.59
AVERAGE(3, 4)	0.65	0.43	TM3*TM4	0.72	0.52
AVERAGE(2, 4)	0.75	0.57	TM1*TM1	0.51	0.44
AVERAGE(1, 4)	0.71	0.50	TM2*TM2	0.62	0.46
AVERAGE(3, 2)	0.51	0.26	TM3*TM3	0.41	0.47
AVERAGE(3, 1)	0.51	0.26	TM4*TM4	0.78	0.53
AVERAGE(2, 1)	0.58	0.34			

comparisons of different models by means of coefficients of determination, and the R^2 has an obvious improvement (Figure 4). This approach has been proved to be successful in Lake Chagan, giving the regression equation seen

$$y = 5.2715x + 2.0052 \quad \left(R^2 = 0.75\right) \tag{1}$$

where y is the logarithmic chl-*a*, and x is the logarithmic ratio of spectral reflectance at 700 and 670 nm.

3.3 Evaluation of Landsat TM data

The broad bands of TM data cannot spectrally resolve the prominent spectral features due to chl-*a* absorption. The chl-*a* absorption at red region of 670 nm is only half contained in the red band of TM data; the peak near 700 nm is totally out of TM red band (see Table III). This means that it is impossible to estimate chl-*a* from TM bands similarly to the use of field spectral regression analysis. Therefore, different methods should be applied to the TM data to determine the chl-*a* level. Attempts were made to find possible single bands or combinations for the TM data. Previous investigations (Kloiber, Brezonik, Olmanson, & Bauer, 2002; Lathrop, 1992; Lavery, Pattiaratchi, Wyllie, & Hick, 1993) suggested that band combinations including ratios, multiplication and/or average might provide useful relationships, and all were made using averaged pixel digital numbers (DNs). A 3 × 3 pixel window, corresponding to the area of 90 × 90 m, was extracted from the TM image for each of water sampling locations. Linear regression was used to quantify possible existing relationships between chl-*a* and TM bands 1–4 or their combinations (Table IV). The most successful regression was found at the band ratio TM4/TM3 to retrieve chl-*a* concentration for the lake as follows

$$y = 116.98x - 29.709 \quad \left(R^2 = 0.67\right) \tag{2}$$

where y is chl-*a* content (μg/l) and x refers to the ratio of TM4/TM3.

Table V The criteria for assessment of lake eutrophication in Lake Chagan

Trophic state	TSI_M (Shu)	Chl-*a* content (μg/l)
Oligotrophic	≤20	≤1.0
Lower-mesotrophic	≤30	≤2.0
Mesotrophic	≤40	≤4.0
Upper-mesotrophic	≤50	≤10.0
Eutrophic	≤70	≤65.0
Hypereutrophic	≤80	≤160.0
Extremely hypereutrophic	≤100	≤1000.0

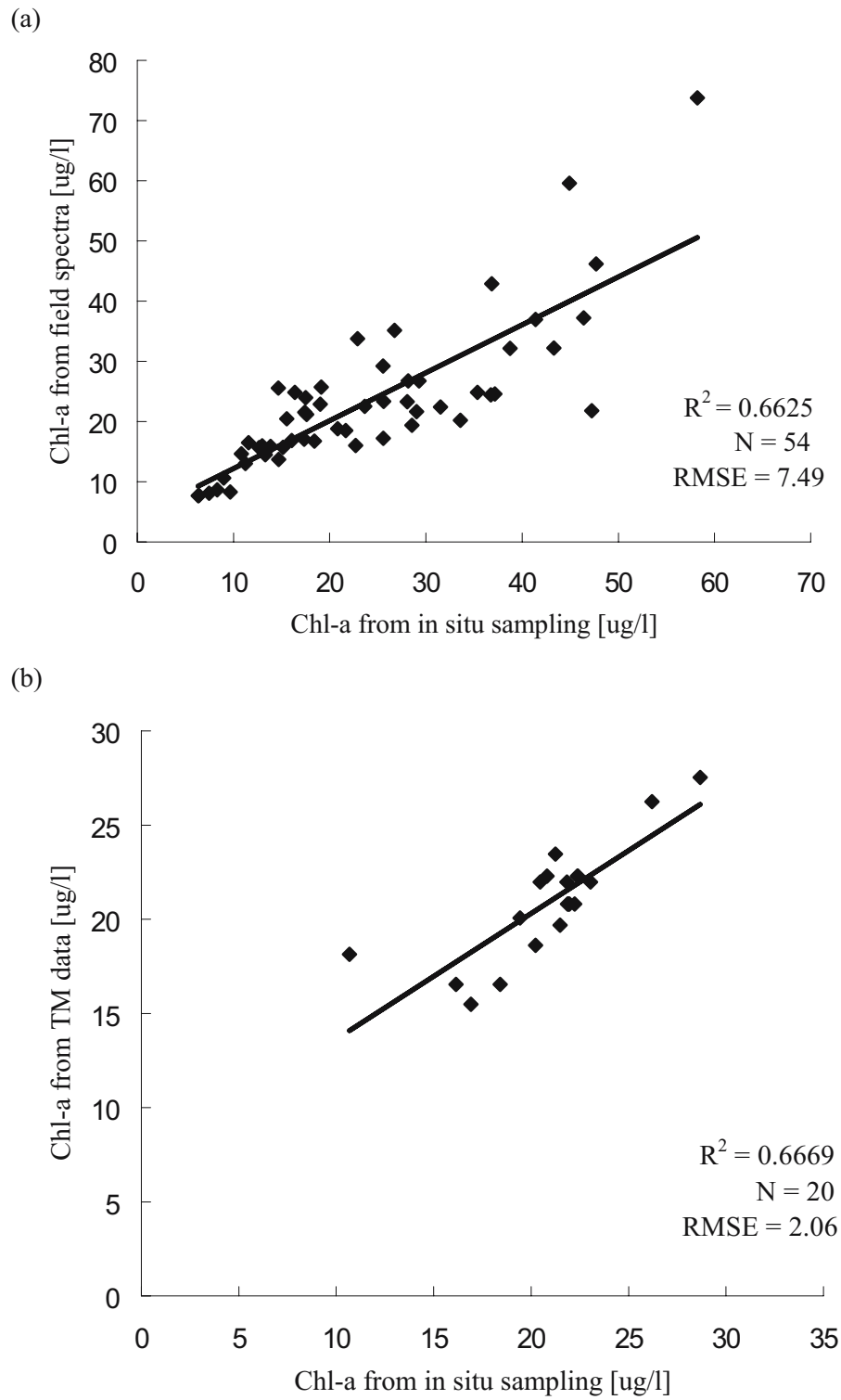

Figure 5 (a) Correlation between chl-*a* as derived from field spectra using the reflectance ratio at 700 and 670 nm and chl-*a* as measured from *in situ* sampling; (b) Correlation between chl-*a* as derived from TM data and chl-*a* as measured from *in situ* sampling in October 2004.

3.4 Estimation of trophic state index for lakes

There are many mathematical methods for the lake eutrophication assessment. The trophic state index (TSI) proposed by Carlson (1977) is the most acceptable method for lake eutrophication evaluation (Xing et al., 2005). As it was mainly based on Secchi disk transparency, the TSI yields continuous values scaled between 0 and 100 for lakes. But it ignores the influence of other factors (e.g., watercolor, dissolved matter and suspended matters) except phytoplankton to Secchi disk transparency (Zhang et al., 2003c). This lack was later repaired by the modified Carlson's TSI_M (Aizaki et al., 1981). However, the assessment methods for the types of the lakes eutrophication also require to suitable for various geo-locations, environment and human activities. Here, we applied the assessment method fitting for the Chinese lakes eutrophication (Shu; 1990, 1993) based on TSI_M as follows

$$\mathrm{TSI_M}(chla) = 10\left(2.46 + \frac{\ln(chla)}{\ln(2.5)}\right) \quad (3)$$

where *chla* means chl-*a* content (μg/l).

The 0–100 scale was divided into the following ranges and each represented a particular trophic state, namely: 0–20 as oligotrophic, 20–30 as lower-mesotrophic, 30–40 as mesotrophic, 40–50 as upper-mesotrophic, 50–70 as eutrophic, 70–80 as hyper-eutrophic, and 80–100 as extremely hypereutrophic status. The assessment standards for each indicator were based on those parameters used in assessing the eutrophication for Chinese Lakes (Shu, 1993; Table V).

4 Results and Discussion

4.1 Chl-*a* from remote sensing data

Figure 5 (a) gives a good correlation between chl-*a* determination from field spectra and *in situ* chl-*a* measurements (R^2 = 0.66) with a root square mean error (RMSE) of 7.49 μg/l. The obtained results showed the lower chl-*a* level at 7–26 μg/l from May to June 2004. It was at the intermediate level of chl-*a* at 15–34 μg/l in August and September, whereas the higher level of chl-*a* from 20 to 74 μg/l existed in July. Clearly, the chl-*a* levels estimated from spectral data are slightly larger than those of *in situ* chl-*a* measurements. But the average of relative errors is less than 20%. So these estimated results are considered effectively. Similarly, Figure 5(b) shows the relationship between chl-*a* derived from TM data and *in situ* measurements. The R^2 is 0.67 with RMSE

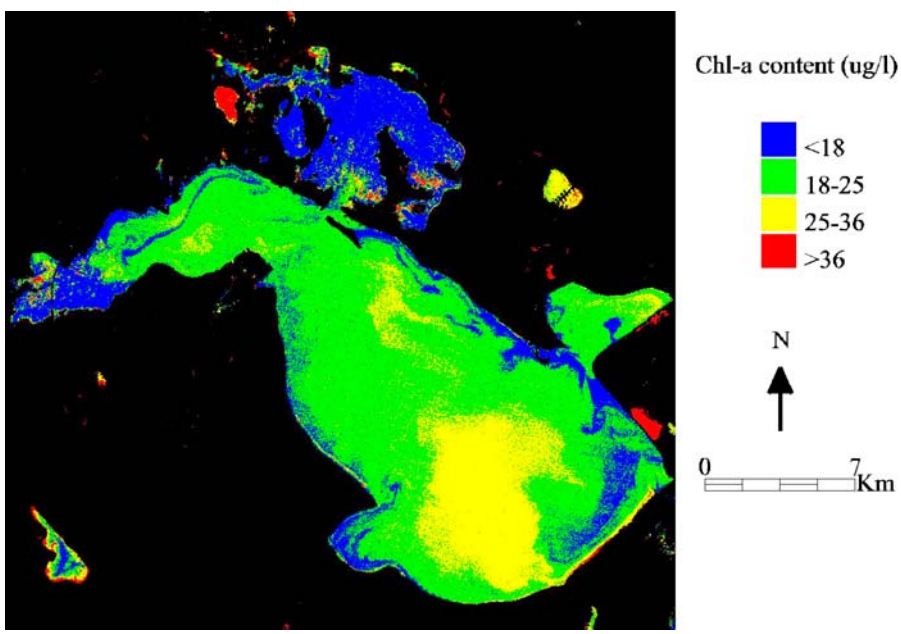

Figure 6 Chl-a content determined from the TM data recorded on 14 October 2004.

of 2.06 μg/l. This result indicates that the TM data could be used to determine chl-*a* levels in Lake Chagan.

Equation (2) was applied to the whole lake surface, producing the density-sliced map from TM data in October 2004 (Figure 6). The highest value of chl-*a* concentration was found in the southern lake, which was very close to Lake Xinmiao with a higher chl-*a* level in October 2004. Since the water of Lake Xinmiao flows into the lake of Chagan through an inlet from the south, the chl-*a* in the southern lake was high up to 25–36 μg/l. Other areas with similar higher amounts of chl-*a* can be observed in the northeastern lake. In comparison, chl-*a* at 18–25 μg/l was found in the middle area of Lake Chagan, while chl-*a* less than 18 μg/l was distributed in the lake borders and the southern area of Lake Chagan from the TM data.

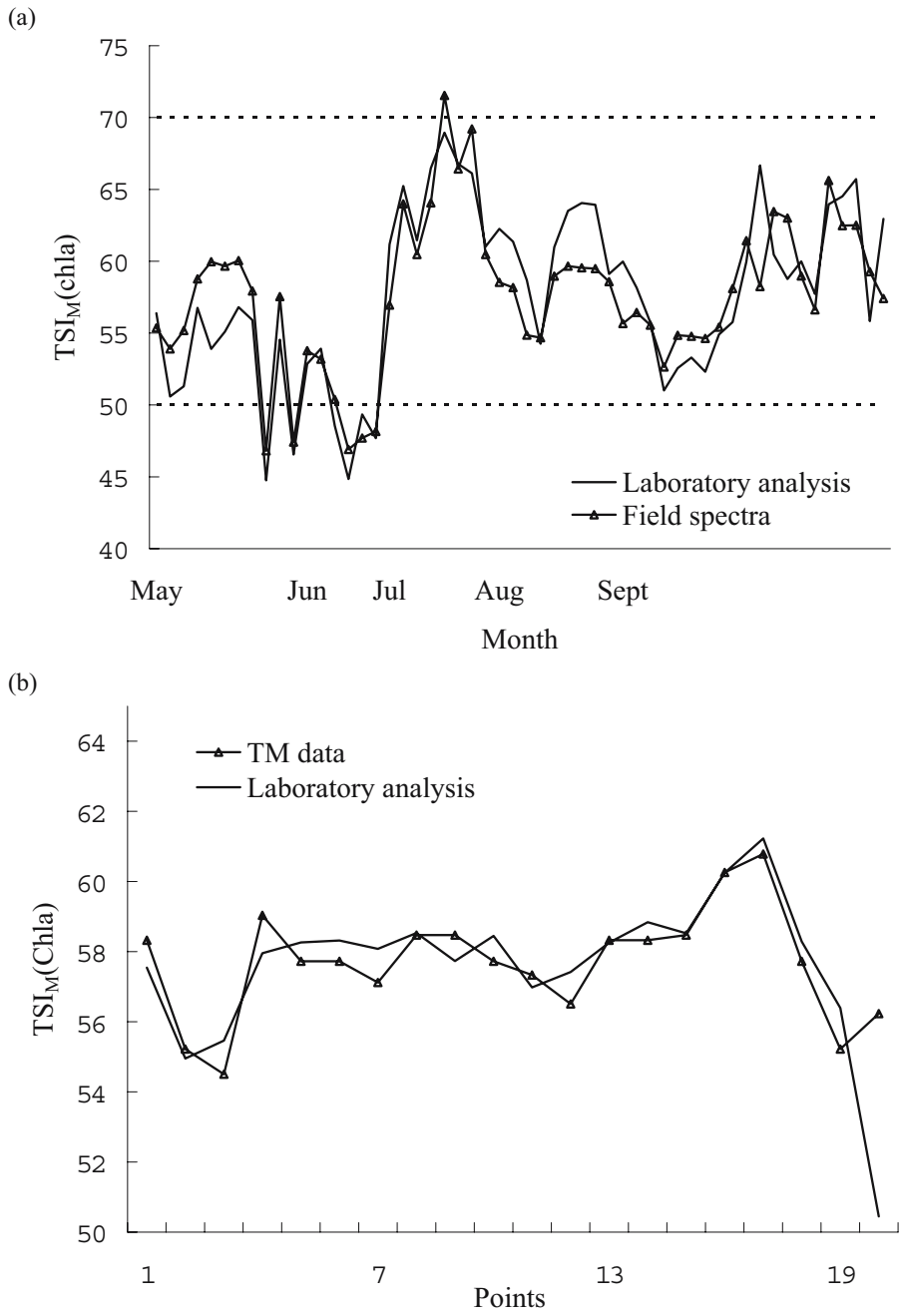

Figure 7 (a) Trophic state index as derived from laboratory analysis and field spectra. (b) Trophic state index as derived from laboratory analysis and TM data in October 2004.

4.2 Trophic state index from field spectra and TM data

Figure 7 indicates the trophic state index as calculated from chl-*a* measurements in the laboratory, chl-*a* determination from field spectra, and chl-*a* estimation from TM data from May to October 2004, respectively. These results were compared with the calculation in all data sets for Lake Chagan. Figure 8(a) gives a high correlation between TSI_M(chla) estimated from field spectra and that from reference data ($R^2 = 0.75$ and RMSE = 2.97 μg/l). Similarly, Figure 8(b) is a

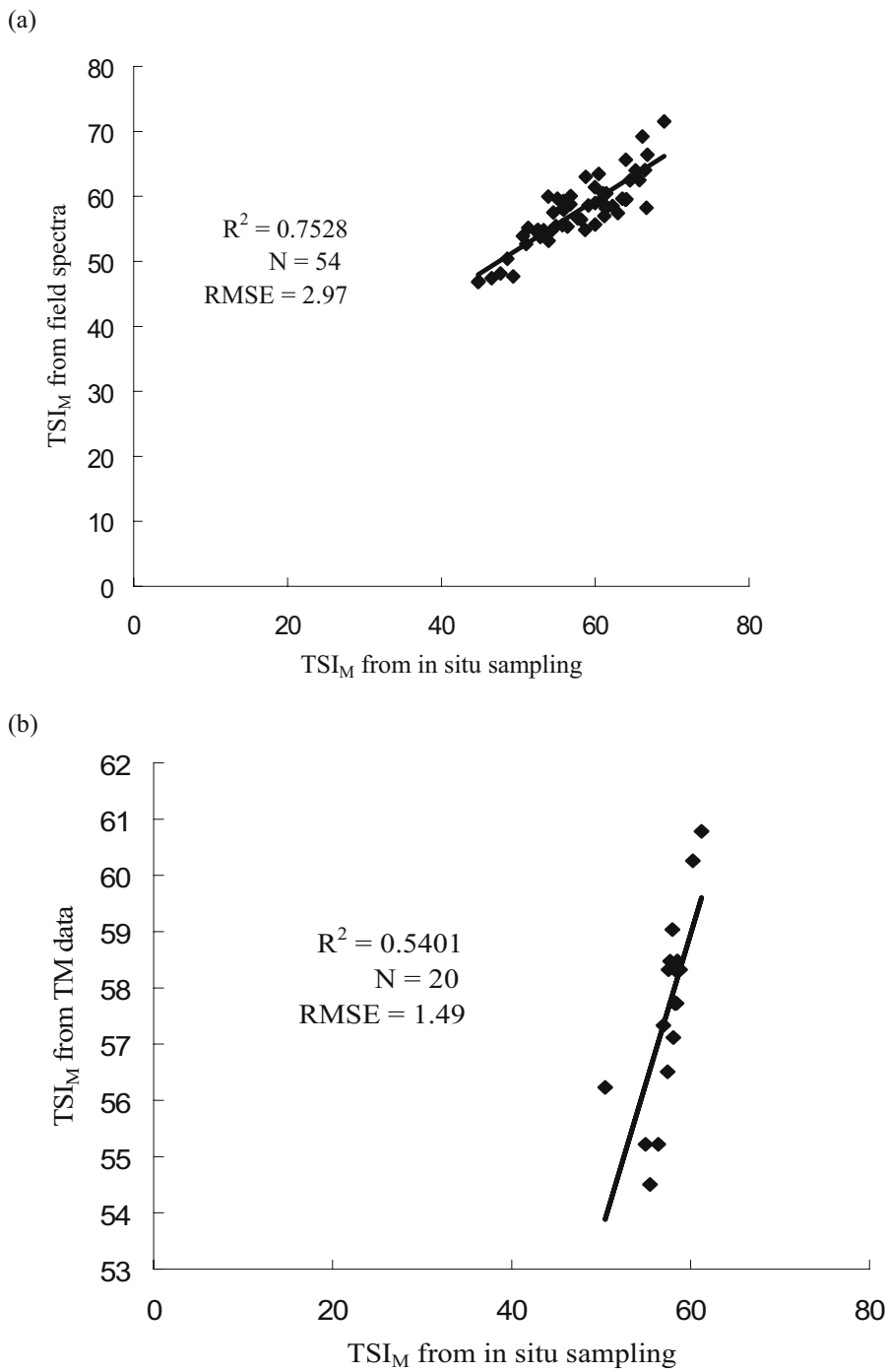

Figure 8 (a) Correlation between TSI_M(chla) as derived from field spectra and TSI_M(chla) as derived from *in situ* sampling. (b) Correlation between TSI_M(chla) as derived from TM data and TSI_M(chla) as derived from *in situ* sampling in October 2004.

reasonable relationship of TSI_M(chla) calculated from TM data with that from reference data ($R^2 = 0.54$ and RMSE = 1.49 μg/l).

All six months from May to October 2004 gave expected results, and their general level and seasonal variation were well represented. Figure 7 shows that TSI_M(chla) increased while chl-*a* increased along with the warmer air temperature. During the summer chl-*a* was apparently increasing, and thus TSI_M(chla) was going up to the maximum in July. As a result, some places were classified into the hypereutrophic state. In contrast, TSI_M(chla) decreased along with the air temperature getting lower and lower from August to October, and therefore TSI_M(chla) examined in

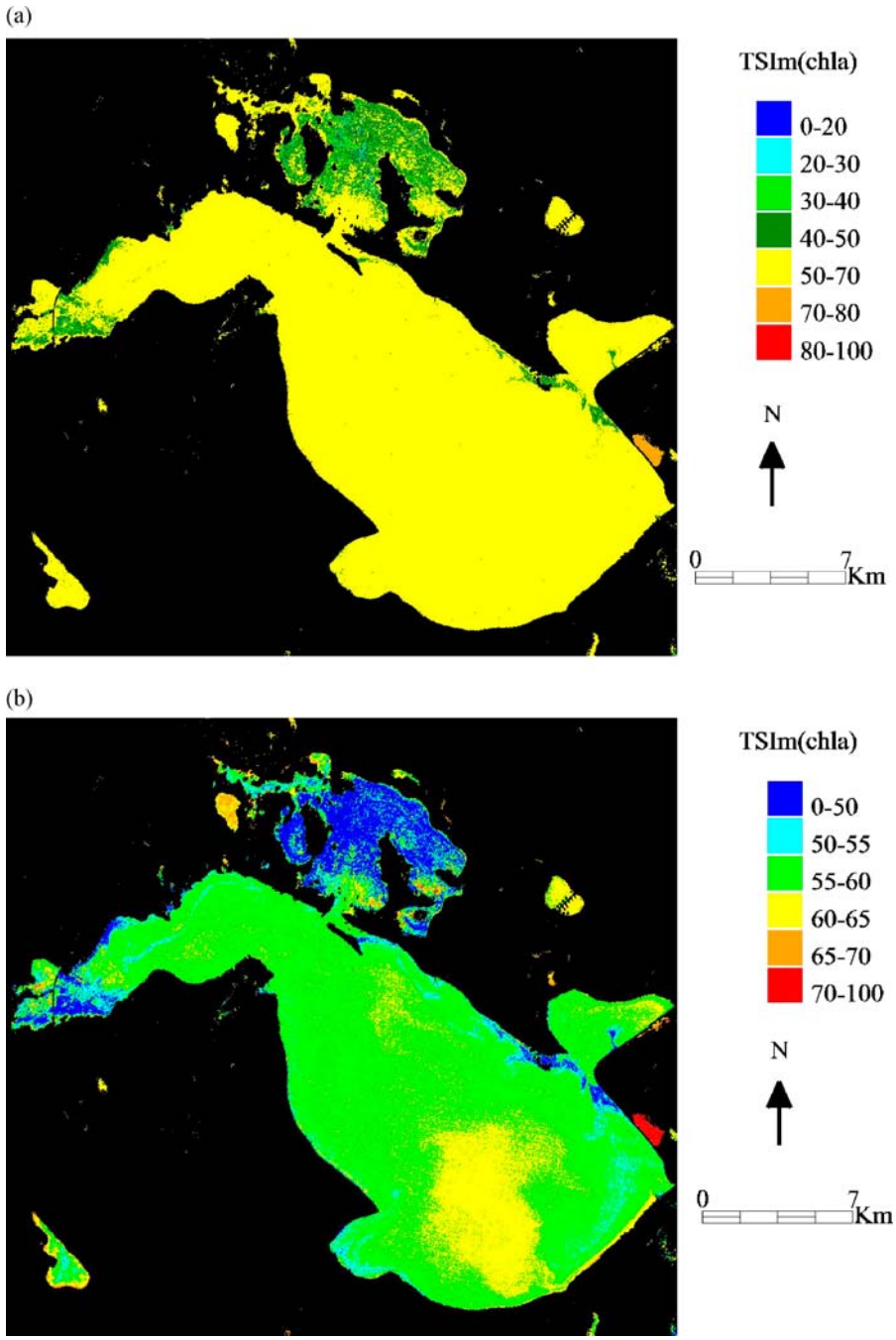

Figure 9 (a) TSI_M(chla) seven classes determined from the TM data recorded on 14 October 2004; (b) TSI_M(chla) four classes (50–70) highlighted from the TM data recorded on 14 October 2004.

October became the lowest in our data sets. From the indictor of TSI_M(chla) in the year of 2004, Lake Chagan was mostly in the eutrophic status, except some small places in the upper-mesotrophic state in May and June. But a few small areas were classified into the hypereutrophic status in July. This means that most of the lake surface can be attributed to the eutrophic state when chl-*a* is also considered (Figure 7 (a) and Figure 9). From the TM image, some pixels at 30–50 were classified as the mesotrophic and upper-mesotrophic state, but none as the hypertrophic status. The eutrophic state at 50–70 could be found in Figure 9(b). Obviously, the TSI_M(chla) distribution of Lake Chagan is close to the chl-*a* distribution due to their same factors. In general, the higher values of TSI_M(chla) at 60–65 can be observed in southern and northeastern lake. The medium TSI_M(chla) at 55–60 can be noted in the middle of Lake Chagan, while the lower TSI_M(chla) at 50–55 is distributed in lake borders and southern lake. Therefore, the results of chl-*a* estimation and the trophic state index determination using Landsat TM and spectral data prove that this is an appropriate method for the assessment of the lake's trophic state in our case study.

5 Conclusions

Landsat-based observations have been presented to evaluate chl-*a* concentration and lake's eutrophication in this study. The obtained results show that Landsat TM and field spectral data can be used effectively to determine chl-*a* levels and the trophic state index in Lake Chagan of Northeastern China. One advantage of using Landsat TM data is to provide the possibility of multi-temporal evaluation over a large coverage with relatively low costs compared to airborne-based measurements and laboratory analysis for the lakes trophic status.

The reflectance spectra in Lake Chagan are generally similar in shape to those from many other lakes with the same trophic state. The comparison of predictive equations shows that some equations [e.g., Equation (1)] are more stable than others, however the logarithmic transformation always improves the estimation accuracy in the study.

Even though the broad spectral bandwidths of Landsat TM data, it is still useful to develop a consistent and reliable relationship of TM bands with chl-*a* concentration. The study shows that TM-estimated reflectance of water presents a good accuracy in TM 1–4 bands or band ratios. In particular, TM4/TM3 gives the best relationship with R^2 of 0.67. The utility of a consistent combination of bands and/or band-ratios helps make the analysis of different satellite-based data comparable. This is an important step towards standardizing the method.

It is proven that the Landsat-based approach is successful in this case study, when compared to the laboratory analysis, field spectral data and TM observations for chl-*a* determination as a basis to calculate the trophic state index for Lake Chagan. Our results confirm that the trophic state of Lake Chagan is eutrophic, in agreement with previous studies using traditional investigations. They highlighted the need for the long-term monitoring of water quality for the lake.

Acknowledgments The authors would like to thank the financial support from the Knowledge Innovation Program of the Northeast Institute of Geography and Agricultural Ecology (NEIGAE), Chinese Academy of Sciences (CAS), and National Natural Science Foundation of China (NSFC) projects (40401003 and 40371082). They also thank the critical comments from two anonymous reviewers to improve the original manuscript.

References

Aizaki, M., Iwakuma, T., & Takamura, N. (1981). Application of modified Carlson's trophic state index to Japanese lakes and its relationship to other parameters related to trophic state. *Research Report on National Institute of Environmental Studies, 23,* 13–31.

Arenz, R. F., Lewis, W. M., & Saunders, J. F. (1996). Determination of chlorophyll and dissolved organic carbon from reflectance data for Colorado reservoirs. *International Journal of Remote Sensing, 17*(8), 1547–1566.

Brezonik, P., Menken, K. D., & Bauer, M. (2005). Landsat-based remote sensing of lake water quality characteristics, including chlorophyll and colored dissolved organic matter (CDOM). *Lake and Reservoir Management, 21* (4), 373–382.

Brivio, P. A., Giardino, C., & Zilioli, E. (2001). Validation of satellite data for quality assurance in lake monitoring applications. *Science of the Total Environment, 268,* 3–13.

Carlson, R. E. (1977). A trophic state index for lakes. *Limnology and Oceanography, 22*(2), 361–369.

Chen, Q., Zhang, Y., Ekroos, A., & Hallikainen, M. (2004). The role of remote sensing technology in the EU water framework directive (WFD). *Environmental Science and Policy, 7*(4), 267–276.

Dekker, A. G. (1993). Detection of optical water parameters for eutrophic lakes by high resolution remote sensing. PhD Dissertation, Free University, Amsterdam.

Dekker, A. G., & Peters, S. W. M. (1993). The use of the thematic mapper for the analysis of eutrophic lakes: A case study in the Netherlands. *International Journal of Remote Sensing, 14*(5), 799–821.

Erkkila, A., & Kalliola, R. (2004). Patterns and dynamics of coastal waters in multi-temporal satellite images: Support to water quality monitoring in the Archipelago Sea, Finland. *Estuarine Coastal and Shelf Science, 60,* 165–177.

Giardino, C., Pepe, M., Brivio, P. A., Ghezzi, P., & Zilioli, E. (2001). Detecting chlorophyll, Secchi disk depth and surface temperature in a sub-alpine lake using Landsat imagery. *Science of the Total Environment, 268,* 19–29.

Gitelson, A. A., Garbuzov, G., Szilagyi, F., Mittenzway, K. H., Karnieli, A., & Kaiser, A. (1993). Quantitative remote sensing methods for real-time monitoring of inland waters quality. *International Journal of Remote Sensing, 14*(7), 1269–1295.

Gitelson, A. A., & Kondratyev, K. Y. (1991). Optical models of mesotrophic and eutrophic water bodies. *International Journal of Remote Sensing, 12,* 373–385.

Gordon, H. R. (1979). Diffusive reflectance of the ocean: The theory of its augmentation by chlorophyll-*a* fluorescence at 685 nm. *Applied Optics, 18,* 1161–1166.

Harma, P., Vepsalainena, J., Hannonena, T., Pyhalahti, T., Kamari, J., Kallio, K., et al. (2001). Detection of water quality using simulated satellite data and semi-empirical algorithms in Finland. *Science of the Total Environment, 268*, 107–121.

Iwashita, K., Kudoh, K., Fujii, H., & Nishikawa, H. (2004). Satellite analysis for water flow of Lake Inbanuma. *Advances in Space Research, 33*(3), 284 – 289.

Kallio, K., Kutser, T., Hannonen, T., Koponen, S., Pulliainen, J., Vepsalainen, J., et al. (2001). Retrieval of water quality from airborne imaging spectrometry of various lake types in different seasons. *Science of the Total Environment, 268,* 59–77.

Kloiber, S. M., Brezonik, P. L., Olmanson, L. G., & Bauer, M. E. (2002). A procedure for regional lake water clarity assessment using Landsat multispectral data. *Remote Sensing of Environment, 82,* 38–47.

Koponen, S., Pulliainen, J., Kallio, K., & Hallikainen, M. (2002). Lake water quality classification with airborne hyperspectral spectrometer and simulated MERIS data. *Remote Sensing Environment, 79,* 51–59.

Koponen, S., Pulliainen, J., Servomaa, H., Zhang, Y., Hallikainen, M., Kallio, K., et al. (2001). Analysis on the feasibility of multisource remote sensing observations for chl-*a* monitoring in Finnish lakes. *Science of the Total Environment, 268,* 95–106.

Lathrop, R. G. (1992). Landsat Thematic Mapper monitoring of turbid inland water quality. *Photogrammetric Engineering and Remote Sensing, 58,* 465– 470.

Lavery, P., Pattiaratchi, C., Wyllie, A., & Hick, P. (1993). Water quality monitoring in estuarine waters using the Landsat Thematic Mapper. *Remote Sensing of Environment, 46,* 268–280.

Ostlunda, C., Flinka, P., Strombeckb, N., Piersonb, D., & Lindell, T. (2001). Mapping of the water quality of Lake Erken, Sweden, from imaging spectrometry and Landsat Thematic Mapper. *Science of the Total Environment, 268,* 139–154.

Porcella, D. B., Peterson, S. A., & Larsen, D. P. (1980). Index to evaluate lake restoration. *Journal of the Environmental Engineering Division ASCE, 106*(EE6), 1151–1169.

Pulliainen, J., Kallio, K., Eloheimo, K., Koponen, S., Servomaa, H., Hannonen, T., et al. (2001). A semi-operative approach to lake water quality retrieval from remote sensing data. *Science of the Total Environment, 268,* 79–93.

Ritchie, J. C., Cooper, C. M., & Schiebe, F. R. (1990). The relationship of MSS and TM digital data with suspended sediments, chlorophyll, and temperature in Moon Lake, Mississippi. *Remote Sensing of Environment, 33,* 137–148.

Shu, J. H. (1990). Discussion of assessment methods of eutrophication in main lakes of China. *Environmental Pollutions and Control, 12*(5), 2–7 (in Chinese).

Shu, J. H. (1993). Assessment of eutrophication in main lakes of China. *Oceanologia et Limnologia Sinica, 24*(6), 616–620 (in Chinese).

Thiemann, S., & Kaufmann, H. (2000). Determination of chlorophyll content and trophic state of lakes using field spectrometer and IRS-1C satellite data in the Mecklenburg Lake District, Germany. *Remote Sensing of Environment, 73,* 227–235.

Walker, W. W. (1979). Use of hypolimnetic oxygen depletion rate as a trophic state index for lakes. *Water Research, 15* (6), 1463–1470.

Wang, Y. P., Xia, H., Fu, J., & Sheng, G. Y. (2004). Water quality change in reservoirs of Shenzhen, China: Detection using LANDSAT/TM data. *Science of the Total Environment, 328,* 195–206.

Xing, K. X., Guo, H. C., Sun, Y. F., & Huang, Y. T. (2005). Assessment of the spatial–temporal eutrophic character in the Lake Dianchi. *Journal of Geographical Sciences, 15* (1), 37– 43.

Xu, F. L., Shu, T., Dawson, R. W., & Li, B. G. (2001). A GIS-based method of lake eutrophication assessment. *Ecological Modelling, 144,* 231–244.

Zhang, Y., Koponen, S., Pulliainen, J., & Hallikainen, M. (2002). Application of an empirical neural network to surface water quality estimation in the Gulf of Finland using combined optical data and microwave data. *Remote Sensing of Environment, 81*(2–3), 327–336.

Zhang, Y., Koponen, S., Pulliainen, J., & Hallikainen, M. (2003a). Application of empirical neural networks to chlorophyll-*a* estimation in coastal waters using remote optosensors. *IEEE Sensors Journal, 3*(4), 376–382.

Zhang, Y., Koponen, S., Pulliainen, J., & Hallikainen, M. (2003b). Water quality retrievals from combined Landsat TM and ERS-2 SAR data in the Gulf of Finland. *IEEE Transactions on Geoscience and Remote Sensing Letters, 41*(3), 622–629.

Zhang, Y., Koponen, S., Pulliainen, J., & Hallikainen, M. (2003c). Empirical algorithms for Secchi disk depth using optical and microwave remote sensing data from the Gulf of Finland and the Archipelago Sea. *Boreal Environment Research, 8*(3), 251–261.

Zibordi, G., Melin, F., Berthon, J. F. (2006). A time series of above-water radiometric measurements for coastal water monitoring and remote sensing product validation. *IEEE Transactions on Geoscience and Remote Sensing Letters, 3*(1), 120–124.